Observation of Asymmetric Stark Profiles from Plasmas Created by a Picosecond KrF Laser

C. H. Nam, W. Tighe, and S. Suckewer
Plasma Physics Laboratory, Princeton University, Princeton, New Jersey 08544

J. F. Seely and U. Feldman
E. O. Hulburt Center for Space Research, Naval Research Laboratory, Washington, D.C. 20375

and

L. A. Woltz
Center for Radiation Research, National Bureau of Standards, Gaithersburg, Maryland 20899
(Received 21 September 1987)

High-resolution extreme-ultraviolet spectra from solid targets irradiated by a picosecond KrF laser focused to 10^{16} W/cm^2 have been recorded. The line profiles of transitions in Li-like fluorine and oxygen are asymmetric and up to 2 Å in width. Calculations indicate the presence of transitions of the type $2p$-$3p$ and other forbidden Stark components.

PACS numbers: 32.70.Jz, 32.70.−n, 52.40.Nk, 52.50.Jm

Highly charged ions produced by the focusing of picosecond-duration laser pulses onto gaseous targets have been reported.[1,2] In this Letter, we present the first high-resolution extreme-ultraviolet spectra obtained by the interaction of powerful picosecond laser pulses with solid targets. The targets were composed of elements with atomic numbers in the range $Z=3$ to $Z=26$ and were irradiated with a KrF laser with a pulse duration of 1.2 psec focused to an intensity of 10^{16} W/cm^2. The spectra in the range 6 to 370 Å were recorded by a 3-m grazing-incidence spectrograph[3] with a resolving power sufficient to observe the line profiles of transitions in highly charged ions.

Picosecond and subpicosecond laser pulses with power 20–30 GW and focused power density 10^{16}–10^{17} W/cm^2 (and larger in the near future) can be used to study ions in extremely high electromagnetic fields. The electric field in the laser focus is comparable with the Coulomb field that binds the electrons to the nucleus, and expected processes include the shift of atomic energy levels and spectral line broadening, the generation of intense extreme-ultraviolet and x-ray radiation, and multiphoton processes.

The KrF laser used in the present experiment is part of a larger system which is being constructed for the development of short-wavelength x-ray lasers and which in-

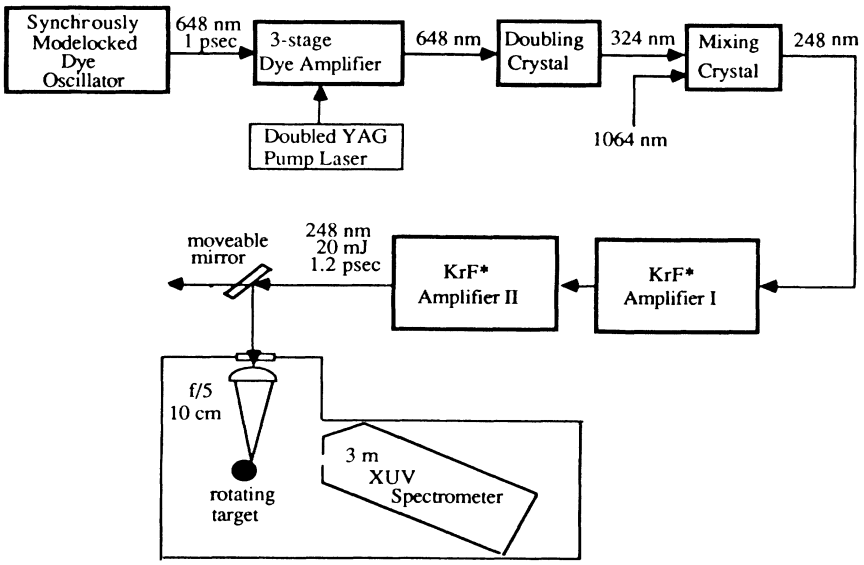

FIG. 1. Schematic of the experiment.

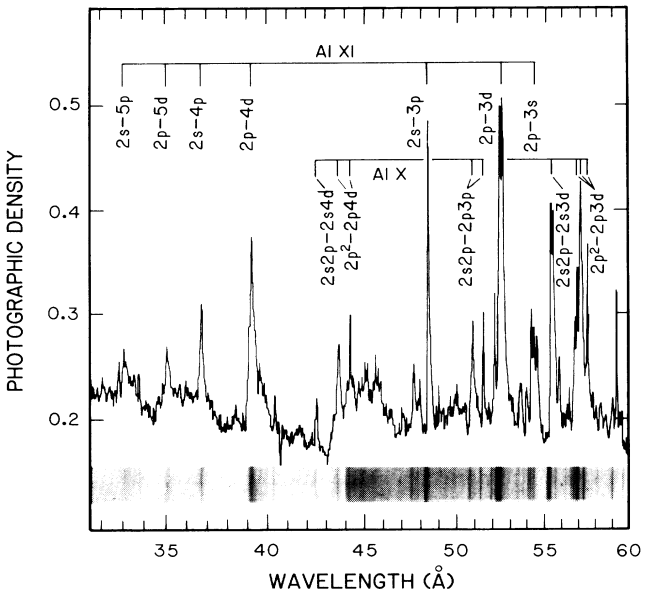

FIG. 2. Densitometer trace of the spectrum from an aluminum target showing transitions in Li-like Al XI and Be-like Al X. A photograph of the spectrum is shown below the densitometer trace.

cludes a CO_2 laser (1-kJ energy, 10–30-nsec pulse duration).[4] A detailed description of this system will be published elsewhere. A schematic of the present experiment is shown in Fig. 1. The master oscillator was a cavity-dumped dye laser tuned to a wavelength of 648 nm. The dye laser was both actively and passively mode locked and produced 1-psec pulses. The dye laser was pumped by the frequency-doubled output of a mode-locked yttrium aluminum garnet (YAlG) laser. The output of the dye laser was injected into a three-stage dye amplifier that was also pumped by the frequency-doubled YAlG laser. The amplified 648-nm pulses were frequency doubled and were mixed with 1064-nm YAlG pulses. The resulting 248-nm pulses were injected into two KrF* amplifiers. The amplified pulses typically had an energy of 20 to 25 mJ and a duration of 1 to 1.2 psec. The pulses were focused by an f/5 spherical lens to an intensity of approximately 10^{16} W/cm^2. The focus was optimized by observation of the signal from an x-ray diode and by examination of the crater size with a microscope.

The laser pulses were incident on a cylindrical target at an angle of 30° to the target normal. The spectrograph viewed the focal spot at an angle of 60° to the target normal, and the entrance slit of the spectrograph was 20 cm from the target. The spectra were recorded on Kodak 101 photographic plates, and the spectra produced by up to 7000 laser shots were integrated onto each exposure. The target was rotated to a new position before each laser shot.

The targets were composed of the elements of interest or were coated with target material. The spectrum from a solid aluminum target is shown in Fig. 2. Isolated aluminum transitions from low stages of ionization, such as the Ne-like $n=2$-3 transitions, were observed to have linewidths less than 100 mÅ. These transitions occur in the low-density expansion plasma, and the linewidths of these transitions are consistent with the 30-mÅ instrumental broadening (resulting from the 10-μm entrance slit) and Doppler source broadening. The much larger widths of the Li-like $n=2$-5 transitions shown in Fig. 2

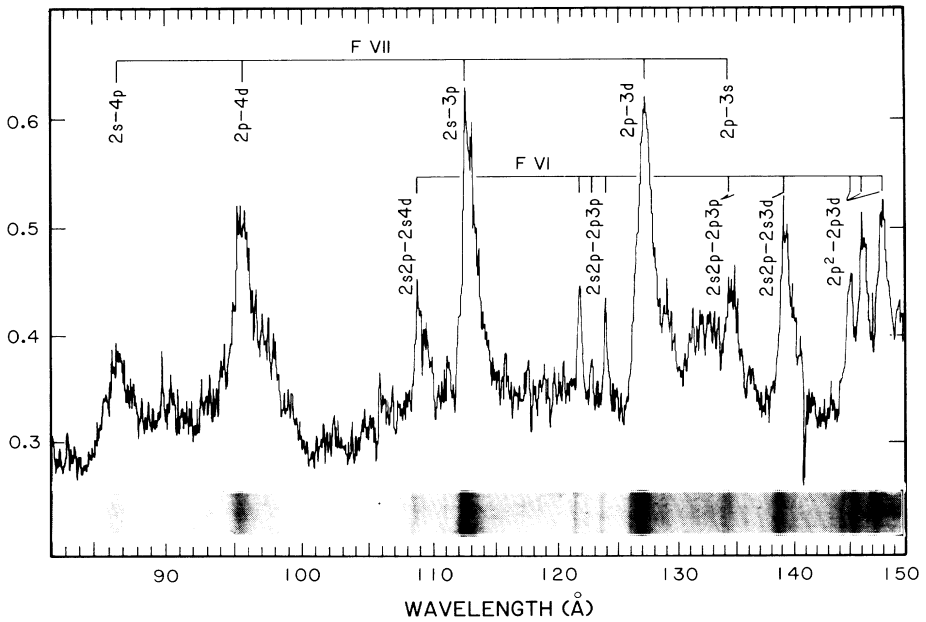

FIG. 3. Densitometer trace of the spectrum from a Teflon target showing transitions in Li-like F VII and Be-like F VI.

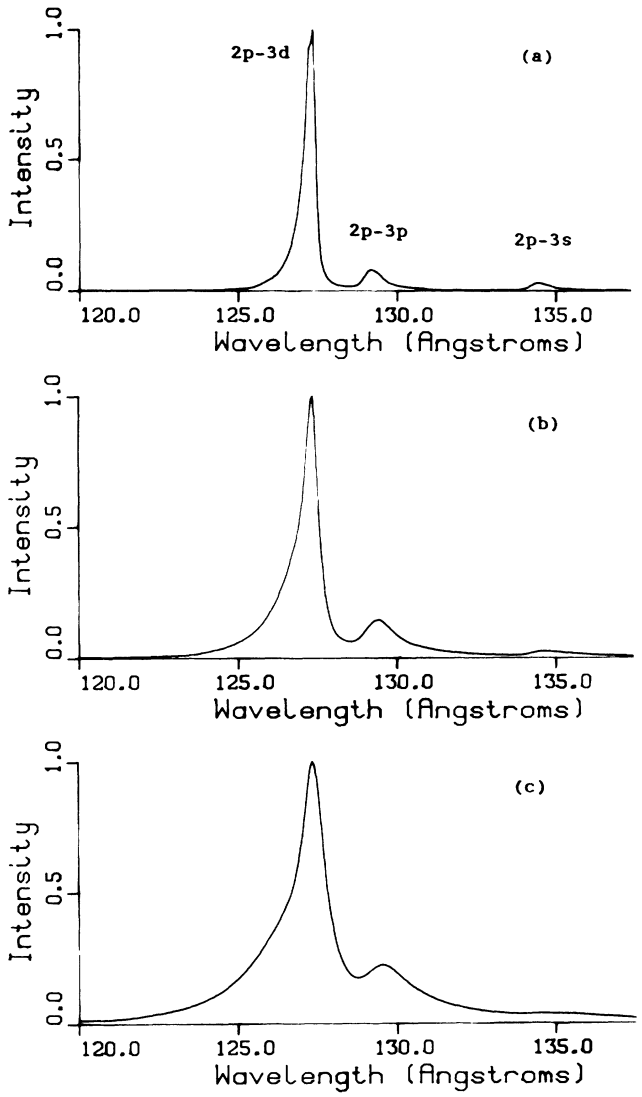

FIG. 4. Calculated F^{6+} Stark profiles for an electron temperature of 500 eV and electron densities of (a) 2×10^{21} cm^{-3}, (b) 5×10^{21} cm^{-3}, and (c) 1×10^{22} cm^{-3}. The $2p$-$3p$ forbidden component appears at 129 Å.

are consistent with quasistatic ion Stark broadening at an electron density in the range 10^{21}–10^{22} cm^{-3}. The same transitions in Li-like fluorine from a Teflon target are shown in Fig. 3. These line profiles are asymmetric and are up to a 2 Å in width. Similar line profiles were observed for Li-like oxygen from a nylon target. Compared with the widths of the aluminum transitions, the Stark widths of the fluorine and oxygen transitions are larger because of the smaller atomic numbers of these elements and the longer wavelengths of the transitions.

It is well known that the microfield due to the plasma ions can cause shifts of the energy levels of emitting ions.[5] In dense plasma, when the shifts become comparable with the energy-level splittings, the wave functions of neighboring states become mixed, and this permits transitions that are not allowed in the absence of the microfield. The parity selection rule breaks down, and normally forbidden transitions between states with the same parity are possible. The ratio of the intensities of the forbidden and allowed transitions increases with plasma density.

Forbidden Stark components have long been observed in neutral emitters.[6] We now show that the asymmetric profiles of the Li-like F^{6+} transitions observed in the present experiment result from forbidden components. The predicted wavelengths[7] of the forbidden $2p$-$3p$ transitions (129.385 and 129.504 Å) are slightly longer than the wavelengths of the allowed $2p$-$3d$ transitions (127.656 and 127.806 Å), and the forbidden component appears as a feature on the red wing of the allowed component.

The line profiles were modeled with a formalism developed for the calculation of spectral line profiles of multielectron ions in dense plasmas.[8] The calculation was done with the quasistatic ion approximation in which the plasma ions that perturb the emitting ion are assumed to have negligible motion during the lifetime of the excited state. A quantum-mechanical relaxation theory was used to calculate the plasma electron broadening of the spectral lines. The atomic energy levels and radial matrix elements were calculated with the atomic-structure program of Cowan.[9] The microfield probability distributions were calculated with the programs of Tighe and Hooper.[10] The excited levels were assumed to have Boltzmann populations.

The calculated profile of the F^{6+} $2p$-$3d$ spectral feature is shown in Fig. 4. At electron densities greater than 5×10^{21} cm^{-3}, the $2p$-$3p$ forbidden component contributes significantly to the red wing of the spectral feature. This is consistent with the enhanced red wing of the observed $2p$-$3d$ spectral feature shown in Fig. 3. Similarly, the red wing of the observed $2p$-$4d$ feature is enhanced by the $2p$-$4p$ forbidden component. The calculated line profiles are weak functions of electron temperature.

The linewidth and asymmetry of the observed F^{6+} $2p$-$3d$ spectral feature are consistent with an electron density of approximately 10^{22} cm^{-3}. This density is comparable with the critical electron density (2×10^{22} cm^{-3}) for 248-nm laser radiation and is much smaller than the target density (4×10^{23} cm^{-3}). Since the plasma expansion during the picosecond laser pulse is negligible, it is likely that the observed emission occurs in the expanding plasma immediately after the laser pulse. During this time, the ion microfield is 1 order of magnitude weaker than the oscillating field of the laser beam (3×10^{9} V/cm) that exists during the laser pulse, and the contribution of the ion microfield to the time-integrated line broadening is apparently dominant because of its longer duration.

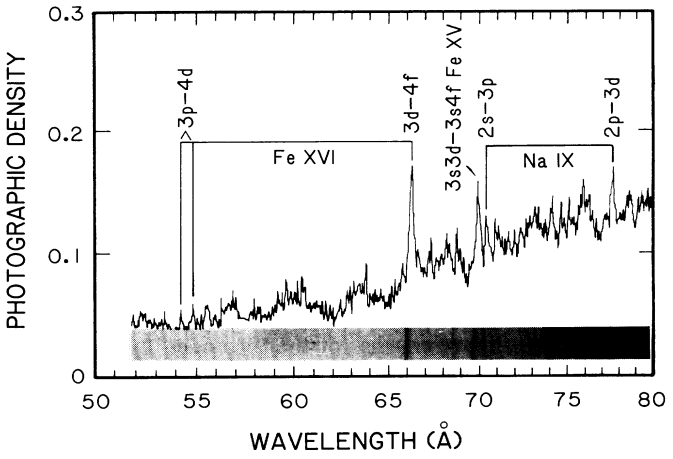

FIG. 5. Densitometer trace of the spectrum of an iron target with surface contamination of sodium. Identified are transitions in Li-like Na IX, Na-like Fe XVI, and Mg-like Fe XV.

The consideration of the times required for electron collisional ionization and radiative decay also indicates that the broad line emission occurs immediately after the laser pulse. For an electron density of 10^{22} cm^{-3}, the time for the electron energy distribution to relax to a Maxwellian is much less than a picosecond. The time for collisional ionization to F^{6+} is approximately 1 psec, and the time for $n=2$-3 collisional excitation is less than a picosecond.[11] The times for the radiative transitions $3p \rightarrow 2s$ and $3d \rightarrow 2p$ are 20 and 6 psec, respectively, and are much larger than the laser pulse duration. Thus the excited F^{6+} ions are formed during the picosecond laser pulse, and the bulk of the emission occurs after the laser pulse. The F^{5+} ionization energy is 160 eV and the F^{6+} $n=2$-3 excitation energy is 100 eV, and it is possible that multiphoton (nonresonance) processes, requiring a large number of 248-nm (5 eV) photons, contribute to the formation of excited F^{6+} during the laser pulse.

The spectrum from an iron target is shown in Fig. 5. The surface of this target was contaminated with sodium, and the Li-like sodium lines are observed to be narrow. A target coated with 1500 Å of LiF was also irradiated, and the F^{6+} lines from the coating were observed to be narrow. This implies that the broad Li-like fluorine lines observed from solid targets do not originate in such a thin surface layer. A thin surface layer of target material may be evaporated by a weak prepulse of amplified spontaneous emission, and the role of the amplified spontaneous emission prepulse, as well as the opacity of the plasma, will be the subject of future work using layered targets. We also note in Fig. 5 the presence of Na-like Fe^{15+} lines, and this represents the most highly charged ion produced in plasmas created by a picosecond laser. The He-like $1s^2\,{}^1S_0$-$1s2p\,{}^1P_1$ resonance line of aluminum at 7.757 Å (1.6-keV excitation energy) was identified in the spectra from the aluminum targets.

We thank C. F. Hooper for suggesting the calculation of the Stark profiles and H. Furth, V. L. Jacobs, R. Kulsrud, and E. Valeo for helpful discussions. We also thank W. E. Behring, C. M. Brown, J. Houston, and J. Robinson for assisting with the experiment. This work was supported by the U.S. Department of Energy Advanced Energy Project of Basic Engineering Sciences, Contract No. KC-05-01, and by the U.S. Office of Naval Research and Strategic Defense Initiative Organization Contract No. N0001487.

[1]T. S. Luk *et al.*, Phys. Rev. Lett. **51**, 110 (1983).
[2]A. L'Huillier *et al.*, Phys. Rev. Lett. **48**, 1814 (1982).
[3]W. E. Behring, R. J. Ugiansky, and U. Feldman, Appl. Opt. **12**, 528 (1973).
[4]S. Suckewer *et al.*, J. Phys. (Paris), Colloq. **47**, C6-23 (1986).
[5]H. R. Griem, *Spectral Line Broadening by Plasmas* (Academic, New York, 1974).
[6]H. R. Griem, Astrophys. J. **154**, 1111 (1968).
[7]L. A. Vainshtein and U. I. Safronova, Phys. Scr. **31**, 519 (1985).
[8]L. A. Woltz and C. F. Hooper, to be published.
[9]R. D. Cowan, *The Theory of Atomic Structure and Spectra* (University of Chicago Press, Berkeley, CA, 1981).
[10]R. J. Tighe and C. F. Hooper, Phys. Rev. A **19**, 2421 (1978).
[11]I. I. Sobelman, L. A. Vainshtein, and E. A. Yukov, *Excitation of Atoms and Broadening of Spectral Lines* (Springer-Verlag, New York, 1981), p. 218.

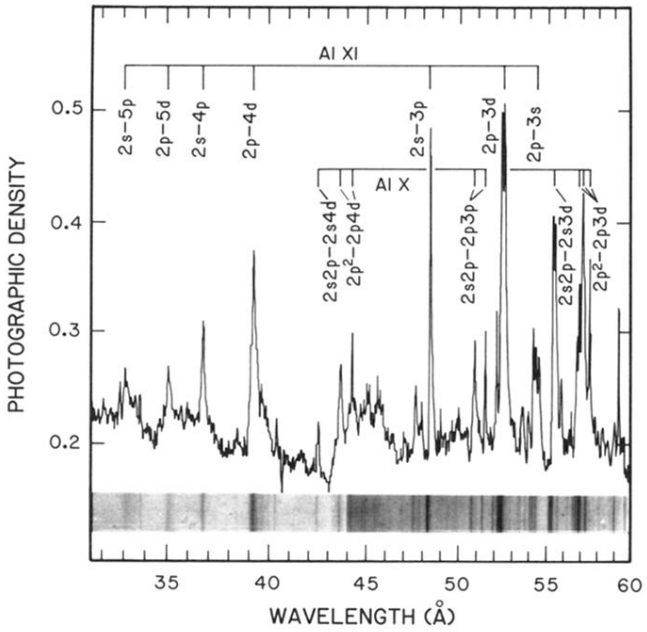

FIG. 2. Densitometer trace of the spectrum from an aluminum target showing transitions in Li-like Al XI and Be-like Al X. A photograph of the spectrum is shown below the densitometer trace.

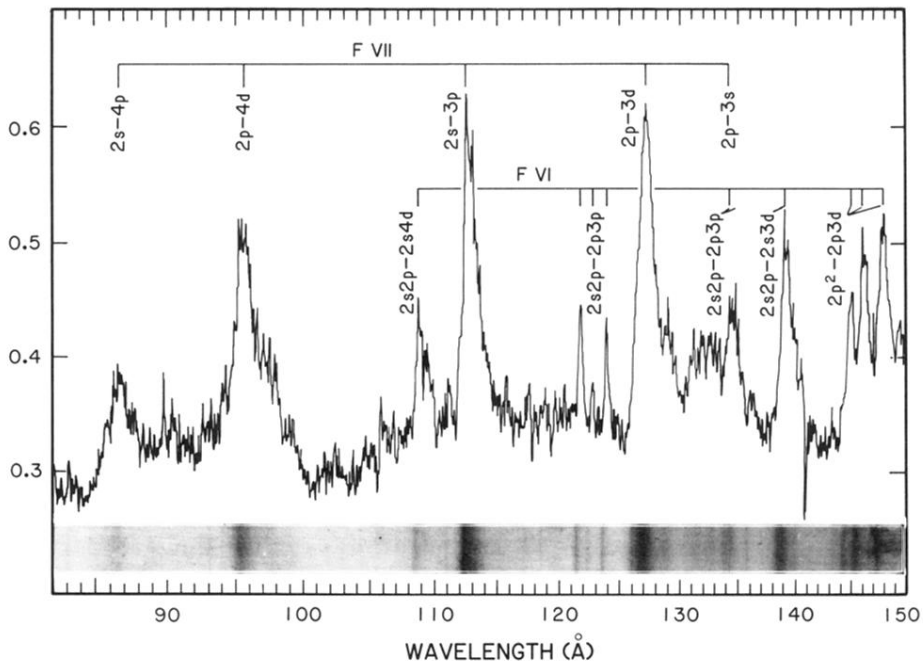

FIG. 3. Densitometer trace of the spectrum from a Teflon target showing transitions in Li-like F VII and Be-like F VI.

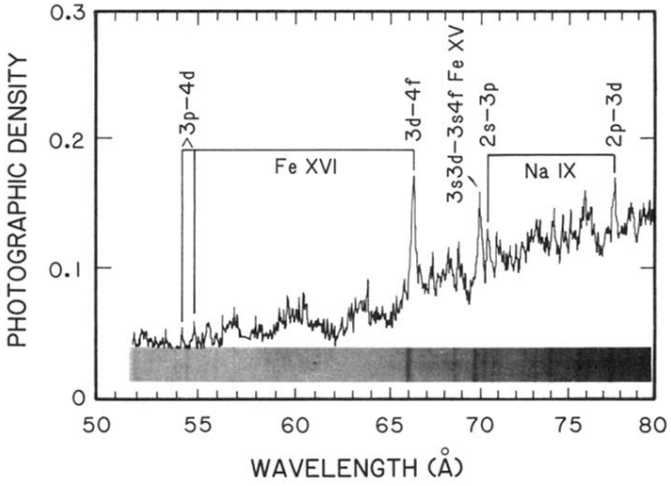

FIG. 5. Densitometer trace of the spectrum of an iron target with surface contamination of sodium. Identified are transitions in Li-like Na IX, Na-like Fe XVI, and Mg-like Fe XV.